

1 **Biological hydrogen storage and release through multiple cycles of bi-**
2 **directional hydrogenation of CO₂ to formic acid in a single process unit**

3

4 Fabian M. Schwarz¹, Jimyung Moon¹, Florian Oswald¹ and Volker Müller^{1,2,*}

5

6 ¹ Department of Molecular Microbiology and Bioenergetics, Institute of Molecular

7 Biosciences, Johann Wolfgang Goethe University, 60438 Frankfurt am Main, Germany

8 ² Lead contact

9 * Correspondence: vmueller@bio.uni-frankfurt.de

10

11

12 **Summary**

13 Hydrogen is a promising fuel in a carbon-neutral economy and many efforts are currently
14 undertaken to produce hydrogen. One of the challenges is a safe and easy way to store and
15 transport the highly explosive gas. One option that is intensively analyzed by chemists and
16 biologists is the conversion of hydrogen and CO₂ to the liquid organic hydrogen carrier formic
17 acid. Here, we demonstrate for the first time that a bio-based system, using the bacterium
18 *Acetobacterium woodii* as biocatalyst, allows multiple cycles of bi-directional hydrogenation
19 of CO₂ to formic acid in a single bioreactor. The process was kept running over two weeks
20 producing and oxidizing 330 mM formic acid in sum. Unwanted side product formation in form
21 of acetic acid was prevented through metabolic engineering of the organism. The demonstrated
22 process design can be considered as a future “bio-battery” for the reversible storage of electrons
23 in form of H₂ in the versatile compound formic acid.

24

25

26

27

28

29

30 **Keywords:** carbon capture, hydrogen storage, whole-cell catalysis, acetogenic bacteria,
31 fermentation, bioreactor, hydrogenation of CO₂, formate oxidation, hydrogen-dependent CO₂
32 reductase

33 **Introduction**

34 Concerns about climate change and global warming have prompted research to replace fossil-
35 fuel based energy carriers with the coincident need to maintain the world's energy demand.¹⁻³
36 Molecular hydrogen has been considered as an attractive, alternative energy carrier which can
37 be produced environmentally friendly and renewable. If the applied hydrogen is produced from
38 renewable energy sources (i.e., solar-, wind-, hydro-, geothermal power) by water splitting and
39 not *via* traditional routes such as steam reforming and partial oxidation of coal, oil and natural
40 gas, no net CO₂ is generated in the production process.⁴⁻⁶ Furthermore, hydrogen is a strong
41 candidate for energy/electricity storage in an environment with excess renewable energy
42 supply. However, due to handling and storage concerns of the highly volatile H₂ gas, the
43 catalytic process of direct hydrogenation of CO₂ has attracted more and more attention in recent
44 years.⁷⁻⁹ The process does not only allow hydrogen energy conversion and storage on a large
45 scale, it further provides a feasible avenue for carbon dioxide capture and storage. The
46 necessary CO₂ molecule can be derived from sources such as industrial flue gas but direct
47 carbon capture and storage (CCS) technologies also enable CO₂ capture from air; a technology
48 that is intensively studied but still requires optimization.¹⁰⁻¹² The process of hydrogen-
49 dependent CO₂ reduction allows the conversion and storage of H₂ and CO₂ in the versatile
50 compound formic acid/formate that is one likely product of the mentioned process.^{9,13,14} Formic
51 acid does not only belong to the group of liquid organic hydrogen carriers (LOHCs), moreover,
52 the compound fulfills the necessary requirements for a putative sustainable formate
53 bioeconomy in future.¹⁵ The field of applications for renewably produced formic acid is diverse
54 since formic acid can be used as bulk chemical, microbial feedstock or can even be applied
55 directly in formic acid fuel cells (DFAFC).¹⁵⁻¹⁷

56 Chemical catalysts can also facilitate the interconversion of H₂ and CO₂ to formic acid,
57 however, mostly requiring noble metals and/or extreme conditions in the reaction process which

58 make the conversion economically unattractive.^{13,18,19} But aside from chemical catalysts, also
59 biological solutions arise. Recently, a soluble, biotechnological interesting enzyme complex
60 was identified in the obligate anaerobic group of acetogenic bacteria, named as hydrogen-
61 dependent CO₂ reductase (HDCR).^{20,21} The enzyme complex consists of four subunits,
62 harboring a [FeFe]-hydrogenase, a molybdenum/tungsten-*bis* pyranopterin guanosine
63 dinucleotide (Mo/W-*bis* PGD) cofactor containing formate dehydrogenase as well as two
64 electron transferring subunits (Figure 1). So far, the HDCRs were purified from the mesophilic
65 and thermophilic acetogenic bacteria *Acetobacterium woodii* and *Thermoanaerobacter kivui*,
66 respectively, but bioinformatic analysis of available genome data indicates the presence of
67 HDCR-like enzymes also outside of this bacterial group.^{20,21} The purified and characterized
68 HDCR enzymes catalyze the direct hydrogenation of CO₂ to formic acid with remarkable
69 catalytic rates, outcompeting chemical catalysts under comparable moderate reaction
70 conditions.²² Noteworthy, the activity is fully reversible and can be affected by the substrate
71 concentrations and prevailing reaction conditions, thus, facilitating the release of stored
72 hydrogen in another catalytic dehydrogenation reaction. The two challenging reactions of
73 hydrogen-dependent CO₂ reduction to formate as well as the “reverse reaction” of formate-
74 driven H₂ production are catalyzed with almost identical catalytic rates.^{20,21} Since the purified
75 enzyme is sensitive to O₂, a HDCR-based whole-cell system was established in serum bottle
76 and bioreactor scale, again, demonstrating the remarkable bi-directionality of the HDCR-based
77 system.^{20,23-25} In the applied system, the HDCR reaction was decoupled from the Wood-
78 Ljungdahl pathway (WLP) of CO₂ fixation by lowering the intracellular amount of ATP using
79 specific inhibitors or ionophores. Here, the antibiotic monensin was identified to be a cheap
80 and efficient uncoupler of the *A. woodii* bioenergetics. The substance works as a carboxylic
81 ion-selective ionophore (especially Na⁺/H⁺ antiporter) which facilitates electroneutral,
82 monovalent ion transport across the cell membrane. Therefore, the substance destroys the Na⁺
83 gradient across the cytoplasmic membrane that drives ATP synthesis in *A. woodii*. Without

84 cellular ATP, the ATP-dependent further conversion of formic acid to acetic acid in the WLP
85 of acetogenic bacteria is blocked (Figure 1). As a result, the typical intermediate formic acid
86 which is produced by many acetogens transiently during acetogenesis from H₂ and CO₂
87 becomes the predominant product.

88 So far, hydrogen-dependent CO₂ reduction to formate as well as formate/formic acid driven H₂
89 and CO₂ production were only studied separately from each other. In this study, we describe
90 and implement a new process design for biological hydrogen storage and release through
91 multiple cycles of bi-directional hydrogenation of CO₂ to formic acid in one single bioreactor
92 by using the same biocatalyst.

93

94 .

95 **Results**

96 **Multiple cycles of bi-directional hydrogenation of CO₂ to formic acid in a single bioreactor**

97 Since the upscaling feasibility of the HDCR-based whole-cell system was recently proven in
98 stirred-tank bioreactors (STR),²⁵ the same bioreactor type was chosen in this study to
99 investigate the bi-directional hydrogenation of CO₂ to formic acid in a single bioreactor by
100 using our established whole-cell system from *A. woodii*. A H₂ storage period (day period) of
101 8 h and a H₂ production period (night period) of 16 h were assumed in the experiment to
102 simulate potential H₂ production times by solar power *via* solar panels. This ratio was based on
103 the fact that in southern Germany the average hours of sunshine during summer time are about
104 7-8 h, thereby, resulting in a time period of 8 h to force hydrogen-dependent CO₂ reduction to
105 formic acid. In the remaining time period (16 h), the produced formic acid was aimed to be re-
106 oxidized to release the stored H₂. To test whether H₂ storage is bi-directional in one bioreactor,
107 non-growing, resting cells suspended in buffer were used. These cells convert substrates to
108 products with high rates but are not able to grow since essential nutrients are missing. *A. woodii*
109 cells were grown in 20 L complex medium with fructose to the end of the exponential growth
110 phase and resting cells were prepared. The bioreactor contained 50 mM K-phosphate buffer at
111 pH 7.0 with additional 15 μM of the metabolic uncoupler monensin that blocks further
112 reduction of formic acid to acetic acid by the cell (Figure 1).²⁵ The pH was kept in the range of
113 5.9 to 8.1 by titration with NH₄OH or H₃PO₄. The experiment was started by adding resting
114 cells to a final cell protein concentration of 1 mg/mL to the bioreactor which was flushed with
115 H₂, CO₂ and N₂. As expected, resting cells immediately started to produce formic acid from H₂
116 and CO₂ with a production rate of 4.3 (± 1.6) mmol g⁻¹ h⁻¹ (Figure 2A).

117 During the “day-period” of 8 h, 28 mM formic acid were produced *via* direct hydrogenation of
118 CO₂. Then, the gas composition was switched to 100% N₂ in the “night period”; by sparging
119 with 100% N₂ the chemical equilibrium was pushed towards hydrogen formation from formic

120 acid (Figure 2B). Formic acid oxidation proceeded with a rate of 2.3 (\pm 0.8) mmol g⁻¹ h⁻¹.
121 During the 16 h “night period”, the formic acid concentration decreased from initial 28 mM to
122 4.9 mM. The formic acid-driven gas production in the “night period” as well as the H₂-
123 dependent CO₂ reduction in the “day-period” could also be observed in the off-gas flow rate.
124 Here, only a qualitative but not quantitative plot can be shown for the off-gas (Figure 2C). This
125 is owed to the used bioreactor set-up since a 1.5 L headspace was applied in the bioreactor to
126 allow potential foaming. Additionally, a low gas-flow rate of 10 mL/min was applied to reduce
127 gas wasting and gas dilution during H₂ production. The applied set-up allowed a diffusive back
128 mixing of the head space additional to a prolonged mean retention time of the gases which
129 distorted the data for quantitative analysis. Nevertheless, the qualitative plot clearly showed
130 that the off-gas flow was reduced during the day period due to H₂ and CO₂ consumption. In
131 contrast, more gas was released from the bioreactor in the night period due to formic acid-
132 driven H₂ and CO₂ production. The effect of alternating gas mixtures, mainly based on varying
133 CO₂ concentrations, could also be seen in the pH profile (Figure 2D). Prior to cell
134 supplementation, CO₂ saturation was achieved in the liquid phase in the bioreactor. Therefore,
135 the initial pH drop was mainly based on the production of formic acid from H₂ and CO₂. After
136 the gas composition was switched to 100% N₂, formic acid was re-oxidized and dissolved H₂
137 as well as CO₂ were flushed out of the reactor. The pH value shifted to more alkaline conditions.
138 In a new cycle of H₂ storage, dissolving CO₂ concentrations as well as formic acid production
139 relocates the pH value to a more neutral state.

140 Since the process enabled the bi-directional storage and release of H₂, the bioreactor application
141 was continued. Over the first 96 h (4 day/night cycles) the reaction kinetics of formic acid
142 formation and formic acid oxidation were monitored (Figure 3A). As can be seen in Figure 3B,
143 the specific activities for both reactions remained almost constant over the time. After 4 cycles,
144 83 and 75% of the initial formic acid formation and formic acid oxidation rate, respectively,
145 were present. Therefore, the system was kept running over 2 weeks which corresponds to 15

146 day/night-cycles or 360 h process time. The amount of produced formic acid per day-period
147 decreased with increasing process time (Figure 4A). At the same time, acetic acid formation
148 increased (Figure 4B). The unwanted side product acetic acid was only produced in traces
149 (around 2 mM) during the first 96 h of fermentation but increased up to 23 mM at the end
150 (t₃₆₀ h). In the last day/night cycle 20% of the initial formic acid formation and formic acid
151 oxidation rate was still present. In sum 330 (± 85) mM formic acid was produced and oxidized
152 by direct hydrogenation of CO₂ within 15 day/night cycles in a single bioreactor. The
153 corresponding pH profile, optical density and total cell protein concentration were also
154 monitored (Figure 4C, D). Here, the optical density decreased slightly at the beginning of the
155 experiments and stayed constant for the rest of the application. As expected, the total cell
156 protein concentration behaved similar to the optical density. Noteworthy, 87% of the initial cell
157 concentration remained after 2 weeks of application, indicating a solid robustness of the
158 *A. woodii* cell system under the given conditions. Moreover, the chosen bioreactor set-up
159 required only 25 mM of phosphoric acid and even no addition of base was needed in the entire
160 process.

161 **Repetitive monensin addition to ensure product specificity**

162 The observed acetic acid formation is not wanted in the process of H₂ storage and H₂ release in
163 and from formic acid. Since acetic acid is only produced from H₂ and CO₂ if the energy state
164 of resting cells is not fully diminished (Figure 1), a putative loss of efficacy over time of the
165 used ionophor monensin was assumed. Therefore, monensin was repetitively added every 72 h
166 to the bioreactor broth. In this approach, the entire bioreactor set-up and the process parameters
167 (gas flow, stirrer speed, gas composition, duration of day/night cycling etc.) were identical to
168 the previous experiment with the exception of the repetitive addition of monensin. The behavior
169 of the bioreactor process as well as product formation were comparable to the previously shown
170 process (Figure S1). Again, formic acid formation was constant for the first 4 day/night cycles,

171 but decreased afterwards whereas acetic acid formation increased. To check whether the
172 bioreactor buffer has still an uncoupling ability due to the presence of sufficient amounts of
173 active monensin, some bioreactor broth was taken at the end of the process to check for its
174 uncoupling ability. Therefore, *A. woodii* cells were removed from the bioreactor broth and the
175 recovered cell-free bioreactor buffer was used for another cell suspension experiment with
176 freshly prepared *A. woodii* cells. No additional monensin was added to the cell-free bioreactor
177 buffer to check its ability to uncouple fresh cells and to force formic acid production. Indeed,
178 the cell-free bioreactor buffer was able to uncouple *A. woodii* cells which showed a specific
179 formic acid production rate of 29 mmol g⁻¹ h⁻¹ (Figure S2). The control experiment with new
180 buffer and added monensin (15 μM) showed a specific activity of 19 mmol g⁻¹ h⁻¹. This clearly
181 shows that the ionophore monensin is still active in the bioreactor broth after 360 h of process
182 time and that other reasons seem to be responsible for the reactivation of the *A. woodii* cell
183 metabolism and the formation of acetic acid.

184 **Genetic modification of *A. woodii* for bi-directional H₂ storage**

185 A gene knock-out of an enzyme in the Wood-Ljungdahl pathway (WLP) for CO₂ reduction to
186 acetic acid was one likely way to prevent the conversion of the formic acid produced to acetic
187 acid and to force formic acid accumulation. Therefore, the genes encoding a central enzyme,
188 the methylene-tetrahydrofolate (THF) reductase, were deleted ($\Delta metVF$). This strain lacks two
189 (*metV*, allocated locus tag Awo_c09300; *metF*, Awo_c09310) of three (*metV*; *metF*; *rnfC2*,
190 Awo_c09290) genes coding for the methylene-THF reductase enzyme complex which
191 catalyzes the formation of a THF-bound methyl group of N⁵-methyl-THF from N⁵,N¹⁰-
192 methylene-THF in the methyl-branch of the WLP (Figure 1).²⁶ The generation, genotype and
193 phenotypic characterization of this mutant will be described elsewhere. If the methylene-THF
194 reductase enzyme is lacking, the further conversion of H₂ and CO₂ to acetate should be blocked.
195 To check for product formation, resting cells of *A. woodii* $\Delta metVF$ were prepared and the

196 conversion of H₂ and CO₂ was investigated in serum bottle experiments in the absence of
197 monensin. Indeed, resting cells of *A. woodii* $\Delta metVF$ converted H₂ and CO₂ exclusively to the
198 end product formic acid (Figure S3A). After 120 min, 12.7 mM formic acid were produced
199 with a specific formic acid formation rate of 18 mmol g⁻¹ h⁻¹ and no acetate could be detected.
200 Also, the “reverse reaction”, formate-driven H₂ production, was studied in resting cells of the
201 $\Delta metVF$ mutant (Figure S3B). When 300 mM of Na-formate were added to the cells, no acetic
202 acid was produced and the oxidation of 167 mM formic acid resulted in the release of 164 mM
203 H₂ after 22 h. The specific H₂ production rate (q_{H_2}) was around 36 mmol g⁻¹ h⁻¹. Next, the bi-
204 directional hydrogenation of CO₂ to formic acid was investigated in a single bioreactor by using
205 resting cells of the *A. woodii* $\Delta metVF$ strain as biocatalysts. The entire process parameters were
206 as before. Resting cells of the $\Delta metVF$ mutant showed a comparable catalytic performance as
207 the *A. woodii* wild type strain (Figure 5). The $\Delta metVF$ mutant was able to produce formic acid
208 from H₂ and CO₂ with a production rate of 3.0 (\pm 0.4) mmol g⁻¹ h⁻¹ during the “day-period”.
209 After 8 h 23 mM formic acid was produced. In the “night period”, the cells oxidized the
210 produced formic acid from the reactor broth with a specific rate of 1.7 (\pm 0.2) mmol g⁻¹ h⁻¹. In
211 16 h, the formic acid concentration decreased to 5.4 mM. As a result of bi-directional
212 hydrogenation of CO₂, 220 (\pm 5) mM of formic acid was produced and oxidized in total in the
213 entire bioreactor process. After 2 weeks of process time, 30% of the initial formic acid
214 formation rate as well as 98% of the initial total cell protein concentration were still present
215 (Figure S4). The entire process consumed 17 mM of phosphoric acid and no base was needed.
216 Noteworthy is that in contrast to wild type cells only traces of acetic acid (0.88 \pm 0.22 mM)
217 were produced after two weeks.

218

219

220 Discussion

221 In this study, we investigated biological hydrogen storage and release in a single bioreactor
222 using *A. woodii* cells as biocatalysts. For this approach, *A. woodii* is superior over, for example,
223 bacteria that use the formate hydrogen lyase (FHL) for formate oxidation. FHL has a strong
224 bias towards formate oxidation, the physiological reaction, whereas the reverse reaction is only
225 possible with appreciable rates under harsh conditions.^{27,28} In contrast, HDCR containing
226 acetogenic bacteria grow on formate²⁹ as well as on H₂ + CO₂ and, therefore, the enzyme must
227 catalyze both reactions with high (identical) rates. Since the equilibrium constant for H₂-
228 dependent CO₂ reduction to formic acid is close to one, minor changes in substrate/product
229 concentrations, pH and temperature can influence the chemical equilibrium. For example,
230 varying gas compositions affected either the production or the degradation of formic acid in our
231 single bioreactor. The observed rates for both reactions were multiple times lower than
232 previously reported rates,²⁵ mainly due to reaction limitations (i.e., substrate limitations) in the
233 bioreactor process. We decided to use a “realistic” and reduced gas flow rate to reduce the gas
234 waste stream and to avoid an excessive dilution of the produced H₂. Additionally, it has to be
235 kept in mind that a change in gas flow rates has an effect on the change in pH values due to the
236 contribution of CO₂. Of course, in a more applied process, the non-captured H₂ and CO₂ of the
237 day-period can be recycled and can be fed back into the bioreactor.

238 Alternatively, air-captured CO₂ or captured and stored CO₂ in form of bicarbonate can be used
239 as CO₂ source in our process in the future. Previously, it was shown that resting cells of
240 *A. woodii* convert KHCO₃ and H₂ into formic acid.²⁰ This conversion is possibly due to the
241 presence of a fast and soluble carbonic anhydrase enzyme which catalyzes the interconversion
242 of bicarbonate in CO₂ and H₂O.³⁰ *A. woodii* cells even showed the highest carbonic anhydrase
243 activity of different investigated acetogens.³¹ In such an approach, the necessary bicarbonate
244 can be obtained from a process called carbon capture and storage by mineral carbonation

245 (CCSM). In this route of CO₂ sequestration, CO₂ is stored in the form of bicarbonate by
246 carbonation of carbonate minerals.^{32,33}

247 The demonstrated bioreactor set-up in this study allowed multiple cycles of bi-directional
248 interconversion of formic acid and H₂/CO₂. Interestingly, the uncoupling effect of monensin on
249 *A. woodii* cells could not be maintained over the whole process time. Since *A. woodii* cells
250 started to produce acetic acid from H₂ and CO₂ in the late phase of the process, Na⁺-dependent
251 energy conservation seemed not to be impaired anymore by addition of monensin. But the loss
252 of function of monensin could be experimentally excluded. The activity of freshly prepared
253 *A. woodii* cells uncoupled by the bioreactor buffer had even more than 100% of the control
254 activity, mainly due to the fact that the re-used bioreactor buffer had a more alkaline pH
255 (pH 7.94) which favors formic acid production. However, acetic acid formation leads to the
256 assumption that *A. woodii* cells may adapt to the antibiotic substance. In general, Gram-positive
257 bacteria are considered to be more sensitive to monensin than Gram-negative bacteria, but
258 monensin adaptation is not a new phenomenon. Pure culture studies of three isolated cattle
259 rumen bacteria have been demonstrated to exhibit a long lag phase prior to growth in the
260 presence of monensin.³⁴ The three investigated Gram-positive bacteria *Enterococcus faecium*,
261 *Enterococcus faecalis* and *Clostridium perfringens* developed monensin resistance through
262 altered cell wall characteristics, showing a thickening of the cell wall or the extracellular
263 polysaccharide (glycocalyx) layer. Similarly, the Gram-positive, amino acid fermenting
264 bacterium *Clostridium aminophilum* could be adapted to monensin.³⁵ It was even shown that
265 adapted cultures can subsequently grow in even higher concentrations of monensin.^{36,37}

266 Another approach to redirect product formation in an organism is by metabolic engineering. In
267 this study, genetic modification of *A. woodii* cells were applied to prevent unwanted side-
268 product formation such as acetic acid in the bioreactor process. The addition of ionophores or
269 antibiotic substances would not be desirable in future demo/pilot scale approaches, therefore,

270 autotrophic acetate formation was blocked by the deletion of the methylene-THF reductase
271 encoding genes. Of course, the knock-out of formyl-THF synthetase genes would be the most
272 obvious way to prevent the further conversion of formic acid in the WLP (Figure 1).
273 Unfortunately, *A. woodii* has two isogenes (*fhs1*, Awo_c09260; *fhs2*, Awo_c08040) encoding
274 formyl-THF synthetases and a double knock-out could, so far, not be obtained.

275 A potential application concept for future bi-directional H₂ storage by using the described
276 bioreactor approach is shown in Figure 6. Excess energy can be used to produce “green” H₂ by
277 water splitting. The necessary renewable energy can be obtained, for example, from sunlight
278 during daytime but other renewable energy sources are also conceivable. H₂ as well as air-
279 captured CO₂ (*via* CCS technologies) can then be converted to the LOHC formic acid in a single
280 bioreactor under ambient pressure and temperature. Here, *A. woodii* cells are used as efficient
281 whole-cell biocatalysts to drive this reaction. The accumulated formic acid can later be re-
282 oxidized in the same bioreactor with the help of the same biocatalyst to release the stored H₂ in
283 times of power deficiencies. The produced H₂ can be separated from the hydrogen-lean CO₂
284 molecule by existing methods for gas separation.^{38,39} CO₂ can be recycled and can afterwards
285 be used in another H₂ storage cycle. Thus, the designed process unit can be considered as a
286 future “bio-battery” for the reversible storage of electrons in form of H₂ in the versatile
287 compound formic acid.

288 The reversible electrocatalysis of a formate dehydrogenase and a hydrogenase from *D. vulgaris*
289 was previously demonstrated using a semiartificial FHL concept.⁴⁰ These systems were
290 immobilized on an electrochemical device to achieve reversible formate/H₂ interconversion.
291 However, the novelty in this study is the shown bi-directionality of the entire process to allow
292 H₂ storage and release over several cycles in a bio-based system. That renewably produced
293 hydrogen *via* water splitting can allow for CO₂ fixation/reduction was previously demonstrated

294 in an inorganic–biological hybrid system using *Xanthobacter autotrophicus* or *Ralstonia*
295 *eutropha*.^{41,42}

296 In summary, we could prove the feasibility of bi-directional hydrogenation of CO₂ to formic
297 acid in a single bioreactor by using our established whole-cell system based on the acetogenic
298 bacterium *A. woodii*. Here, the H₂ and CO₂ stored and captured during the day period could be
299 released in the night period by the same biocatalyst in the same process unit. As far as we know,
300 it is the first time that a bio-based system allows multiple cycles of bi-directional
301 interconversion of formic acid and H₂/CO₂ in a single bioreactor. This could allow storage of
302 locally produced energy/H₂ in form of the non-toxic, non-environmental harmful LOHC formic
303 acid and release of H₂ in the same environment. The safety concerns as well as the need for
304 valuable raw materials and metals could be less critical compared to already existing energy
305 storage technologies. In future, a switch to less energy intense bioreactor types such as bubble
306 column bioreactors would be the preferred way to improve the total energy balance of the
307 system. Many influencing factors of the investigated process itself but also the dependence from
308 global/local political regulations effects the viability of a process. However, the unique process
309 design described here combines two chemically challenging reactions which could be an
310 integral part of a future hydrogen economy to combat global warming and to solve the
311 renewable energy demand of the growing world population.

312

313

314

315 **Experimental procedures**

316 **Resource availability**

317 *Lead contact*

318 Further information and requests for resources and materials should be directed to and will be
319 fulfilled by the lead contact, Volker Müller (vmueller@bio.uni-frankfurt.de).

320 *Materials availability*

321 The materials in this study will be made available upon reasonable request.

322 *Data and code availability*

323 The datasets generated in this study are available from the lead contact on reasonable
324 request.

325

326 **Organism and cultivation**

327 *Acetobacterium woodii* (DSM 1030) wild type was cultivated at 30 °C under anoxic conditions
328 in carbonate-buffered medium⁴³ using 1 L flasks (Müller-Krempel, Bülach, Switzerland) with
329 500 mL media or in 22 L flasks (Glasgerätebau Ochs; Bovenden-Lenglern, Germany) with 20 L
330 media. The medium was prepared under anoxic conditions as described before.^{44,45} To grow
331 the *A. woodii metVF* deletion strain, 50 mg/l uracil and 50 mM glycine-betaine was added to
332 the medium. Fructose (20 mM) was used as growth substrate for all cultivations and cell growth
333 was followed by measuring the optical density at 600 nm with an UV/Vis spectrophotometer.

334 **Preparation of resting cells and cell suspension experiments**

335 Resting cells of *A. woodii* wilde type and $\Delta metVF$ were prepared as described before.²⁰ In
336 resting cells, biomass formation/cell division does not occur but cells are still fully metabolic
337 active. The cells were washed and resuspended in K-phosphate buffer (50 mM K-phosphate,

338 20 mM KCl, 4 μM resazurin, 2 mM DTE, pH 7.0). The total cell protein concentration of the
339 cell suspension was determined according to Schmidt et al.⁴⁶ and the cells were directly used
340 for the subsequent experiments. To determine the conversion of H₂ + CO₂ into formate by
341 resting cells of *A. woodii*, 120 mL serum bottles (Glasgerätebau Ochs GmbH, Bovenden-
342 Lenglern, Germany) containing pre-warmed buffer (50 mM K-phosphate, 20 mM KCl, 4 μM
343 resazurin, 2 mM DTE, pH 7.0) under a N₂ atmosphere were incubated with cell suspensions at
344 the protein concentration stated. The final liquid volume in the serum flasks was 10 mL and the
345 resting cells were incubated for at least 10 min at 30 °C prior to the start of the experiment. The
346 reaction was started by changing the head space to a H₂ + CO₂ (80:20%, [v/v]) atmosphere with
347 1 bar overpressure. If necessary, the ionophore monensin (as sodium salt; dissolved in EtOH)
348 was added prior to the reaction start and liquid samples were taken over the time to analyze the
349 formation of acetic acid and formic acid.

350 **Multiple cycles of bi-directional hydrogenation of CO₂ to formic acid in a single bioreactor**

351 The bioreactor experiments were carried out in Biostat Aplus bench-top reactors from Sartorius
352 (Melsungen, Germany) with a working volume of 1.5 L as described before.²⁵ Each bioreactor
353 was equipped with micro sparger, baffles, two Rushton-impeller, pH-probe (Hamilton,
354 Bonaduz, Switzerland), temperature probe and a redox potential probe (Hamilton, Bonaduz,
355 Switzerland) (Figure 7). The temperature of the buffer (50 mM K-phosphate, 20 mM KCl,
356 2 mM DTE, pH 7.0) was maintained at 30 °C, using a cooling finger and heating sleeve. The
357 permitted pH-range of the bioreactor experiments was from pH 5.9 to 8.1 and was achieved by
358 titration with H₃PO₄ (4 M) and NH₄OH (4 M). The gas flow rate was maintained during the
359 “day/night cycles” at a constant value of 10 mL/min using a digital mass-flow controller
360 (Bronkhorst High-Tech, Ruurlo, Netherlands). The supplied gas composition varied in the
361 stoichiometry of H₂, CO₂ and N₂ in dependence of the catalytic cycle. During the “day period”
362 (duration: 8 h; H₂ storage process) a gas composition of 45% H₂, 45% CO₂ and 10% N₂ [v/v]

363 was used (Nippon Gases, Germany). During the “night period” (duration: 16 h; H₂ production
364 process) a gas composition of 100% N₂ [v/v] was used. The gas switch was made manually
365 without an interruption of the existing gas flow. The installed micro sparger ensured the
366 formation of microbubbles to enhance mass transfer between gaseous and aqueous phase.⁴⁷ The
367 headspace of the bioreactor was at atmospheric pressure and the gas-liquid mixing was achieved
368 by using a stirrer set-up with two Rushton-impeller at 400 rpm. The bioreactor buffer was
369 prepared under aerobic, non-sterile conditions and oxygen was removed by subsequent
370 sparging with 45% H₂, 45% CO₂ and 10% N₂ [v/v] for about 16 h. After the achievement of
371 anoxic conditions and CO₂ saturation in the liquid phase, 2 mM DTE and 15 μM monensin
372 were added as indicated. The reaction was started by adding *A. woodii* cell suspension to a final
373 cell protein concentration of 1 mg/mL to the bioreactor. Samples (2 mL) were taken at defined
374 time points for product analysis as well as OD and total cell protein determination. A single
375 liquid sample of 3 mL reactor broth was taken and discarded prior to the bioreactor sampling
376 to account for the dead volume of the sampling line. The samples were centrifuged (18,000 × g,
377 8 min, room temperature) to remove cells and the supernatant was frozen at -20 °C until further
378 off-line analysis.

379 **Inhibitory effect of reactor buffer on fresh cell suspensions**

380 Fresh cells suspensions of *A. woodii* were prepared as described in the section above. The
381 reaction buffer for cell suspension experiments was obtained from the bioreactor approach at
382 time point 360 h. Therefore, 60 mL cell suspension of each bioreactor was transferred to a
383 120 mL anoxic serum bottle (Glasgerätebau Ochs GmbH, Bovenden-Lenglern, Germany) at
384 the end of the fermentation process. Afterwards, buffer and cells were separated *via*
385 centrifugation (11,500 × g, 15 min, 4 °C) under anoxic conditions. The supernatant was taken
386 as reaction buffer in the subsequent serum bottle experiment with a total cell protein

387 concentration of 1 mg/mL of the freshly prepared *A. woodii* cells. The serum bottle experiments
388 were performed as described above.

389 **Analytical methods**

390 The concentrations of formic acid and acetic acid were measured by high-performance liquid
391 chromatography using a 1260 Infinity II LC System (Agilent Technologies, Santa Clara, CA,
392 USA) as described before⁴⁸ or by using a commercially available formic acid and acetic acid
393 determination kit (Boehringer Mannheim/R-Biopharm AG, Mannheim/Darmstadt, Germany)
394 following the instructions of the manufacturer. Bioreactor off-gas analysis was conducted *via* a
395 Micro-GC (Inficon, Bad Ragaz, Switzerland) which was equipped with two measurement
396 modules containing different analytical columns. The analytical conditions and columns were
397 used as described before.⁴⁹ The total cell protein concentration of the prepared cell suspensions
398 was determined according to Schmidt et al.⁴⁶

399 **Chemicals**

400 All chemicals were supplied by Sigma-Aldrich (St. Louis, USA) and Carl Roth GmbH & Co
401 KG (Karlsruhe, Germany). All premixed gases for cell suspension experiments were purchased
402 from Nippon Gases Europe (Düsseldorf, Germany). Pure gases such as N₂ (purity of 5.0) were
403 purchased from Air Liquide (Paris, France).

404

405 **Supplemental information**

406 Supplemental information can be found online.

407 **Acknowledgements**

408 This project has received funding from the European Research Council (ERC) under the
409 European Union's Horizon 2020 research and innovation program (grant agreement no
410 741791).

411 Author contributions

412 V.M designed and supervised the research, analyzed the data and wrote the manuscript. F.M.S

413 designed the research, performed the experiments, analyzed the data and wrote the manuscript.

414 J.M. generated the mutant strain. F.O. supervised the fermentation.

415

416 Declaration of interests

417 Goethe-University Frankfurt and V.M possess a patent on the HDCR based whole-cell system

418 for storing gaseous hydrogen through producing methanoate (patent number: EP2816119).

419

420

421

422

423

424 **References**

- 425 1. Veziroğlu, T.N., and Şahin, S. (2008). 21st Century's energy: Hydrogen energy system.
426 Energy Convers. Manage. *49*, 1820–1831. 10.15518/isjaee.2019.04-06.014-027
- 427 2. Bockris, J.O.M. (2013). The hydrogen economy: Its history. Int. J. Hydrogen Energy
428 *38*, 2579-2588. 10.1016/j.ijhydene.2012.12.026.
- 429 3. Singh, S., Jain, S., Venkateswaran, P., Tiwari, A.K., Nouni, M.R., Pandey, J.K., and
430 Goel, S. (2015). Hydrogen: A sustainable fuel for future of the transport sector. Renew.
431 Sustain. Energy Rev. *51*, 623-633. 10.1016/j.rser.2015.06.040.
- 432 4. Holladay, J.D., Hu, J., King, D.L., and Wang, Y. (2009). An overview of hydrogen
433 production technologies. Catal. Today *139*, 244-260. 10.1016/j.cattod.2008.08.039.
- 434 5. Wang, M., Wang, Z., Gong, X., and Guo, Z. (2014). The intensification technologies to
435 water electrolysis for hydrogen production—A review. Renew. Sustain. Energy Rev. *29*,
436 573-588. 10.1016/j.rser.2013.08.090.
- 437 6. Brandon, N.P., and Kurban, Z. (2017). Clean energy and the hydrogen economy. Philos.
438 Trans. Royal Soc. A *375*, 20160400. Artn 20160400
439 10.1098/Rsta.2016.0400.
- 440 7. Wang, W., Wang, S., Ma, X., and Gong, J. (2011). Recent advances in catalytic
441 hydrogenation of carbon dioxide. Chem. Soc. Rev. *40*, 3703-3727.
442 10.1039/C1CS15008A.
- 443 8. Moret, S., Dyson, P.J., and Laurency, G. (2014). Direct synthesis of formic acid from
444 carbon dioxide by hydrogenation in acidic media. Nat. Commun. *5*, 4017.
445 10.1038/ncomms5017.
- 446 9. Preuster, P., Papp, C., and Wasserscheid, P. (2017). Liquid organic hydrogen carriers
447 (LOHCs): toward a hydrogen-free hydrogen economy. Acc. Chem. Res. *50*, 74-85.
448 10.1021/acs.accounts.6b00474.
- 449 10. Lackner, K.S., Brennan, S., Matter, J.M., Park, A.H., Wright, A., and van der Zwaan,
450 B. (2012). The urgency of the development of CO₂ capture from ambient air. Proc. Natl.
451 Acad. Sci. U. S. A. *109*, 13156-13162. 10.1073/pnas.1108765109.
- 452 11. Sanz-Perez, E.S., Murdock, C.R., Didas, S.A., and Jones, C.W. (2016). Direct capture
453 of CO₂ from ambient air. Chem. Rev. *116*, 11840-11876.
454 10.1021/acs.chemrev.6b00173.
- 455 12. Shi, X., Xiao, H., Azarabadi, H., Song, J., Wu, X., Chen, X., and Lackner, K.S. (2020).
456 Sorbents for the direct capture of CO₂ from ambient air. Angew. Chem. Int. Ed. Engl.
457 *59*, 6984-7006. 10.1002/anie.201906756.
- 458 13. Enthaler, S., von Langermann, J., and Schmidt, T. (2010). Carbon dioxide and formic
459 acid-the couple for environmental-friendly hydrogen storage? Energy Environ. Sci. *3*,
460 1207-1217. 10.1039/b907569k.
- 461 14. Eppinger, J., and Huang, K.W. (2017). Formic acid as a hydrogen energy carrier. ACS
462 Energy Lett. *2*, 188-195. 10.1021/acsenerylett.6b00574.
- 463 15. Yishai, O., Lindner, S.N., Gonzalez de la Cruz, J., Tenenboim, H., and Bar-Even, A.
464 (2016). The formate bio-economy. Curr. Opin. Chem. Biol. *35*, 1-9.
465 10.1016/j.cbpa.2016.07.005.
- 466 16. Aslama, N.M., Masdara, M.S., Kamarudina, S.K., and Dauda, W.R.W. (2012).
467 Overview on direct formic acid fuel cells (DFAFCs) as an energy sources. APCBEE
468 Procedia *3*, 33-39.
- 469 17. Kawanami, H., Himeda, Y., and Laurency, G. (2017). Formic acid as a hydrogen
470 carrier for fuel cells toward a sustainable energy system. Adv. Inorg. Chem. *70*, 395-
471 427. 10.1016/bs.adioch.2017.04.002.
- 472 18. Hull, J.F., Himeda, Y., Wang, W.H., Hashiguchi, B., Periana, R., Szalda, D.J.,
473 Muckerman, J.T., and Fujita, E. (2012). Reversible hydrogen storage using CO₂ and a

- 474 proton-switchable iridium catalyst in aqueous media under mild temperatures and
475 pressures. *Nat. Chem.* *4*, 383-388. 10.1038/nchem.1295.
- 476 19. Appel, A.M., Bercaw, J.E., Bocarsly, A.B., Dobbek, H., DuBois, D.L., Dupuis, M.,
477 Ferry, J.G., Fujita, E., Hille, R., Kenis, P.J., et al. (2013). Frontiers, opportunities, and
478 challenges in biochemical and chemical catalysis of CO₂ fixation. *Chem. Rev.* *113*,
479 6621-6658. 10.1021/cr300463y.
- 480 20. Schuchmann, K., and Müller, V. (2013). Direct and reversible hydrogenation of CO₂ to
481 formate by a bacterial carbon dioxide reductase. *Science* *342*, 1382-1385.
482 10.1126/science.1244758.
- 483 21. Schwarz, F.M., Schuchmann, K., and Müller, V. (2018). Hydrogenation of CO₂ at
484 ambient pressure catalyzed by a highly active thermostable biocatalyst. *Biotechnol.*
485 *Biofuels* *11*, 237. 10.1186/s13068-018-1236-3.
- 486 22. Müller, V. (2019). New horizons in acetogenic conversion of one-carbon substrates and
487 biological hydrogen storage. *Trends Biotechnol* *37*, 1344-1354.
488 10.1016/j.tibtech.2019.05.008.
- 489 23. Kottenhahn, P., Schuchmann, K., and Müller, V. (2018). Efficient whole cell biocatalyst
490 for formate-based hydrogen production. *Biotechnol. Biofuels* *11*, 93. 10.1186/s13068-
491 018-1082-3.
- 492 24. Schwarz, F.M., and Müller, V. (2020). Whole-cell biocatalysis for hydrogen storage
493 and syngas conversion to formate using a thermophilic acetogen. *Biotechnol. Biofuels*
494 *13*, 32. 10.1186/s13068-020-1670-x.
- 495 25. Schwarz, F.M., Oswald, F., and Müller, V. (2021). Acetogenic conversion of H₂ and
496 CO₂ into formic acid and *vice versa* in a fed-batch-operated stirred-tank bioreactor. *ACS*
497 *Sustain. Chem. Eng.* *9*, 6810-6820. 10.1021/acssuschemeng.1c01062.
- 498 26. Bertsch, J., Öppinger, C., Hess, V., Langer, J.D., and Müller, V. (2015). Heterotrimeric
499 NADH-oxidizing methylenetetrahydrofolate reductase from the acetogenic bacterium
500 *Acetobacterium woodii*. *J. Bacteriol.* *197*, 1681-1689. 10.1128/JB.00048-15.
- 501 27. Roger, M., Brown, F., Gabrielli, W., and Sargent, F. (2018). Efficient hydrogen-
502 dependent carbon dioxide reduction by *Escherichia coli*. *Curr. Biol.* *28*, 140-145.
503 10.1016/j.cub.2017.11.050.
- 504 28. Roger, M., Reed, T.C.P., and Sargent, F. (2021). Harnessing *Escherichia coli* for bio-
505 based production of formate under pressurized H₂ and CO₂ gases. *Appl. Environ.*
506 *Microbiol.* *87*, e0029921. 10.1128/AEM.00299-21.
- 507 29. Moon, J., Dönig, J., Kramer, S., Poehlein, A., Daniel, R., and Müller, V. (2021).
508 Formate metabolism in the acetogenic bacterium *Acetobacterium woodii*. *Environ.*
509 *Microbiol.* 10.1111/1462-2920.15598.
- 510 30. Steger, F., Reich, J., Fuchs, W., Rittmann, S.K.R., Gubitz, G.M., Ribitsch, D., and
511 Bochmann, G. (2022). Comparison of carbonic anhydrases for CO₂ sequestration. *Int.*
512 *J. Mol. Sci.* *23*. 10.3390/ijms23020957.
- 513 31. Braus-Stromeyer, S.A., Schnappauf, G., Braus, G.H., Gössner, A.S., and Drake, H.L.
514 (1997). Carbonic anhydrase in *Acetobacterium woodii* and other acetogenic bacteria. *J.*
515 *Bacteriol.* *179*, 7197-7200.
- 516 32. Lackner, K.S. (2002). Carbonate chemistry for sequestering fossil carbon. *Annu. Rev.*
517 *Energy Environ.* *27*, 193-232. 10.1146/annurev.energy.27.122001.083433.
- 518 33. Sanna, A., Hall, M.R., and Maroto-Valer, M. (2012). Post-processing pathways in
519 carbon capture and storage by mineral carbonation (CCSM) towards the introduction of
520 carbon neutral materials. *Energy Environ. Sci.* *5*, 7781-7796. 10.1039/C2EE03455G
- 521 34. Simjee, S., Heffron, A.L., Pridmore, A., and Shryock, T.R. (2012). Reversible monensin
522 adaptation in *Enterococcus faecium*, *Enterococcus faecalis* and *Clostridium perfringens*
523 of cattle origin: potential impact on human food safety. *J. Antimicrob. Chemother.* *67*,
524 2388-2395. 10.1093/jac/dks236.

- 525 35. Rychlik, J.L., and Russell, J.B. (2002). The adaptation and resistance of *Clostridium*
526 *aminophilum* F to the butyrylvibriocin-like substance of *Butyrvibrio fibrisolvens* JL5
527 and monensin. FEMS Microbiol. Lett. 209, 93-98. 10.1111/j.1574-
528 6968.2002.tb11115.x.
- 529 36. Morehead, M.C., and Dawson, K.A. (1992). Some growth and metabolic characteristics
530 of monensin-sensitive and monensin-resistant strains of *Prevotella* (Bacteroides)
531 *ruminicola*. Appl. Environ. Microbiol. 58, 1617-1623. 10.1128/aem.58.5.1617-
532 1623.1992.
- 533 37. Callaway, T.R., and Russell, J.B. (1999). Selection of a highly monensin-resistant
534 *Prevotella bryantii* subpopulation with altered outer membrane characteristics. Appl.
535 Environ. Microbiol. 65, 4753-4759. 10.1128/AEM.65.11.4753-4759.1999.
- 536 38. Galizia, M., Chi, W.S., Smith, Z.P., Merkel, T.C., Baker, R.W., and Freeman, B.D.
537 (2017). 50th anniversary perspective: polymers and mixed matrix membranes for gas
538 and vapor separation: a review and prospective opportunities. Macromolecules 50,
539 7809-7843. 10.1021/acs.macromol.7b01718.
- 540 39. Tong, Z., and Sekizkardes, A.K. (2021). Recent developments in high-performance
541 membranes for CO₂ separation. Membranes 11, 156. 10.3390/membranes11020156.
- 542 40. Sokol, K.P., Robinson, W.E., Oliveira, A.R., Zacarias, S., Lee, C.Y., Madden, C.,
543 Bassegoda, A., Hirst, J., Pereira, I.A.C., and Reisner, E. (2019). Reversible and selective
544 interconversion of hydrogen and carbon dioxide into formate by a semiartificial formate
545 hydrogenlyase mimic. J. Am. Chem. Soc. 141, 17498-17502. 10.1021/jacs.9b09575.
- 546 41. Liu, C., Sakimoto, K.K., Colon, B.C., Silver, P.A., and Nocera, D.G. (2017). Ambient
547 nitrogen reduction cycle using a hybrid inorganic-biological system. Proc. Natl. Acad.
548 Sci. U. S. A. 114, 6450-6455. 10.1073/pnas.1706371114.
- 549 42. Liu, C., Colón, B.E., Silver, P.A., and Nocera, D.G. (2018). Solar-powered CO₂
550 reduction by a hybrid biological| inorganic system. J. Photochem. Photobiol. A: Chem.
551 358, 411-415. 10.1016/j.jphotochem.2017.10.001.
- 552 43. Heise, R., Müller, V., and Gottschalk, G. (1989). Sodium dependence of acetate
553 formation by the acetogenic bacterium *Acetobacterium woodii*. J. Bacteriol. 171, 5473-
554 5478. 10.1128/jb.171.10.5473-5478.1989.
- 555 44. Hungate, R.E. (1969). A roll tube method for cultivation of strict anaerobes. In Methods
556 in Microbiology, J.R. Norris, and D.W. Ribbons, eds. (Academic Press), pp. 117-132.
- 557 45. Bryant, M.P. (1972). Commentary on the Hungate technique for culture of anaerobic
558 bacteria. Am. J. Clin. Nutr. 25, 1324-1328. 10.1093/ajcn/25.12.1324.
- 559 46. Schmidt, K., Liaaen-Jensen, S., and Schlegel, H.G. (1963). Die Carotinoide der
560 *Thiorhodaceae*. Arch Mikrobiol 46, 117-126.
- 561 47. Bredwell, M.D., and Worden, R.M. (1998). Mass-transfer properties of microbubbles.
562 1. Experimental studies. Biotechnology progress 14, 31-38. 10.1021/bp970133x.
- 563 48. Schwarz, F.M., Ciurus, S., Jain, S., Baum, C., Wiechmann, A., Basen, M., and Müller,
564 V. (2020). Revealing formate production from carbon monoxide in wild type and
565 mutants of Rnf- and Ech-containing acetogens, *Acetobacterium woodii* and
566 *Thermoanaerobacter kivui*. Microb. Biotechnol. 13, 2044-2056. 10.1111/1751-
567 7915.13663.
- 568 49. Wiechmann, A., Ciurus, S., Oswald, F., Seiler, V.N., and Müller, V. (2020). It does not
569 always take two to tango: "Syntrophy" via hydrogen cycling in one bacterial cell. ISME
570 J. 14, 1561-1570. 10.1038/s41396-020-0627-1.
- 571

572 Figure legends

573 Figure 1. HDCR-based whole-cell catalysis and the bioenergetics and biochemistry of the
574 metabolism in *A. woodii*. The gaseous substrates H₂ and CO₂ can diffuse across the cell
575 membrane where the HDCR enzyme hydrogenates the CO₂ molecule to formic acid. Formic
576 acid is then bound to the cofactor tetrahydrofolic acid and reduced to a methyl group and then
577 condensed with carbon monoxide, derived by reduction of a second molecule of CO₂, and
578 coenzyme A to acetyl-CoA which is further metabolized to acetic acid. If the energy state of
579 the cell is reduced by the ionophore monensin, which destroys the sodium ion potential across
580 the cytoplasmic membrane required for ATP synthesis, the ATP-dependent further conversion
581 of formic acid in the Wood-Ljungdahl pathway (WLP) is blocked. Another way to prevent
582 formic acid conversion to acetic acid is by metabolic engineering. The knock-out of the
583 methylene-THF reductase coding genes prevents further formic acid conversion in the methyl
584 branch of the WLP. The exact mechanism of formic acid uptake and excretion is so far not
585 known. The HDCR enzyme is the key enzyme for HDCR-based whole-cell catalysis to convert
586 H₂ and CO₂ into formate and *vice versa*. HDCR, hydrogen-dependent CO₂ reductase; HydA2,
587 [FeFe]-hydrogenase; FdhF2, molybdenum containing formate dehydrogenase; HycB2/3,
588 electron-transferring subunits; HydABC, electron-bifurcating hydrogenase; CODH/ACS, CO
589 dehydrogenase/acetyl-CoA synthase; THF, tetrahydrofolate; HCO-THF, formyl-THF; HC-
590 THF, methenyl-THF; H₂C-THF, methylene-THF; H₃C-THF, methyl-THF; Rnf,
591 ferredoxin:NAD⁺ oxidoreductase; CoFeSP, corrinoid-iron-sulfur-protein; Fd²⁻, reduced
592 ferredoxin. Transparent pink box indicates the methyl and carbonyl-branch of the WLP.

593

594 Figure 2. Process development during day/night cycles for biological hydrogen storage
595 and release in a single bioreactor. Resting cells were transferred into the bioreactor at a final
596 concentration of 1 mg/ml in K-phosphate buffer (50 mM K-phosphate, 20 mM KCl, 2 mM

597 DTE, pH 7.0). A continuous gas flow rate of 10 mL min⁻¹ with 45% H₂, 45% CO₂ and 10% N₂
598 (day period) or 100% N₂ (night period) was applied. The reaction temperature was kept at 30
599 °C in the liquid phase and the stirrer speed was set at 400 rpm. Monensin (15 μM) was added
600 as uncoupling agent. A) Formate production from H₂ and CO₂ during day period, B) formate
601 oxidation during night period, C) qualitative off-gas graph over the first 48 h and D)
602 corresponding pH course over two day/night cycles. The shown data from the off-gas graph is
603 from one representative experiment out of three independent replicates. All other data points
604 are mean ± SD, N = 3.

605

606 **Figure 3. Kinetics of multiple cycles of bi-directional hydrogenation of CO₂ to formic acid**
607 **in a single process unit.** A) Formic acid formation and formic acid oxidation over 4 day/night
608 cycles in the first 96 h of process time and B) the corresponding specific activity of formic acid
609 production (black bars) and formic acid oxidation (grey bars). 100% of the activity corresponds
610 to a formic acid production rate of 4.3 mmol g⁻¹ h⁻¹. The formic acid oxidation rate of 100% is
611 similar to 2.3 mmol g⁻¹ h⁻¹. All data points are mean ± SD, N = 3.

612

613 **Figure 4. Long-term application of bi-directional interconversion of formic acid and**
614 **H₂/CO₂ in a single process unit.** Shown are A) 15 formic acid formation/oxidation cycles of
615 the entire process (360 h) and B) corresponding side-product formation profile of acetic acid.
616 Additionally, C) optical density at 600 nm, total cell protein concentration and D) pH were
617 monitored over the entire process. Empty triangles up, optical density at 600 nm; empty
618 triangles down, total cell protein concentration. All data points are mean ± SD, N = 3.

619

620 **Figure 5. Multiple cycles of bi-directional hydrogenation of CO₂ to formic acid in a single**
621 **bioreactor using *A. woodii* $\Delta metVF$.** Formic acid formation and formic acid oxidation as well
622 as acetic acid production is shown for two weeks of fermentation with multiple day/night
623 cycles. In total 220 mM formic acid was formed and oxidized. A more detailed process kinetic
624 is shown for the initial day- (blue box) and night-period (green box). The specific formic acid
625 formation and oxidation rate were 3.0 mmol g⁻¹ h⁻¹ and
626 1.7 mmol g⁻¹ h⁻¹, respectively. Triangles, formic acid; squares, acetic acid. All data points are
627 mean \pm SD, N = 3.

628

629 **Figure 6. Schematic cycle of future bi-directional H₂ storage via direct hydrogenation of**
630 **CO₂ to formate using a single bioreactor.** Excess energy generated from renewable sources
631 can be used to produce H₂ by water splitting. Captured CO₂ and H₂ are then converted into the
632 LOHC formate by whole-cell catalysis in a single process unit. The same bioreactor system and
633 biocatalyst are used for overnight hydrogen release from the LOHC system. The produced H₂
634 can ensure off-grid power supply in energy-lean times and CO₂ can be recycled and re-used in
635 another H₂ storage cycle. The use of sunlight is just exemplary and different sources can be
636 used to produce renewable electricity in dependence of the local conditions, therefore, making
637 different scenarios more likely and more beneficial. All icons were taken from freepik from
638 flaticon.com.

639

640 **Figure 7. Scheme of a batch operated stirred-tank bioreactor with continuous gas supply.**
641 Whole- cells of *A. woodii* were used as biocatalysts in a batch operated stirred-tank bioreactor
642 to reversibly convert H₂ and CO₂ into formic acid. During the day period (8 h) a gas
643 composition of 45% H₂ + 45% CO₂ + 10% N₂ was fed into the bioreactor. During the night
644 period (16 h) the gas composition was switched to 100% N₂. pHIRC, pH indicator recording

645 and control; pO₂IRC, pO₂ indicator recording and control; TIRC, temperature indicator
646 recording and control; ORPIR, oxidation reduction potential indicator and recording; GC, gas
647 chromatography.

648

649

650

651

652

653

654

655

656

657

658

659

660

661

662

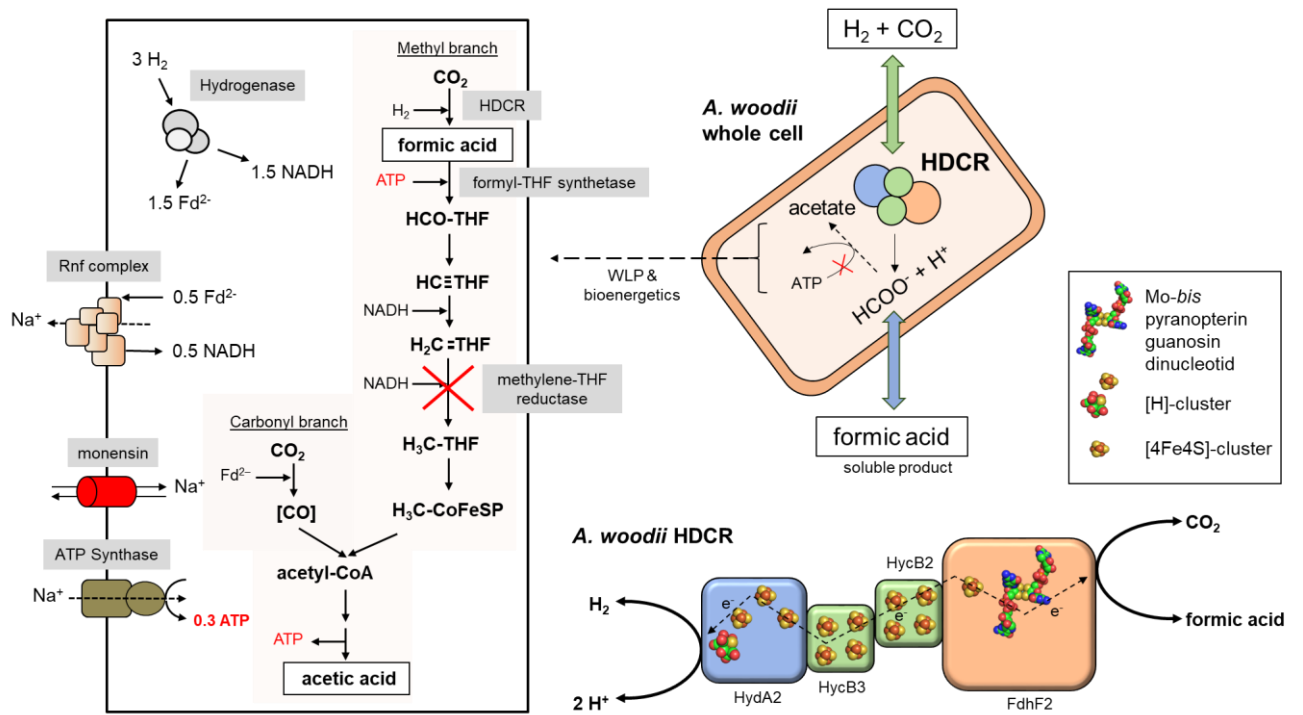
663

664

665 **Figures**

666

667 **Figure 1**



668

669

670

671

672

673

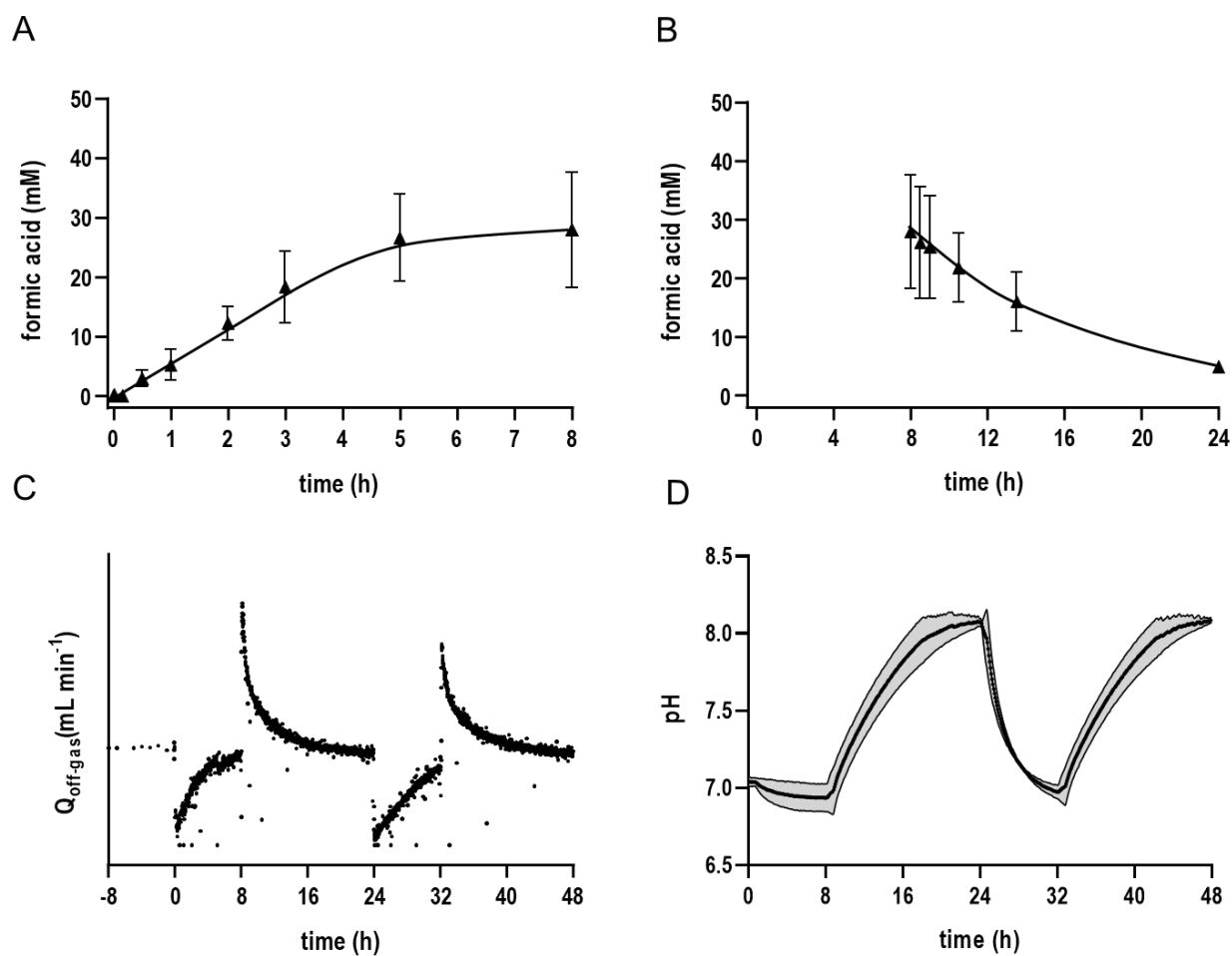
674

675

676

677

678

679 **Figure 2**

680

681

682

683

684

685

686

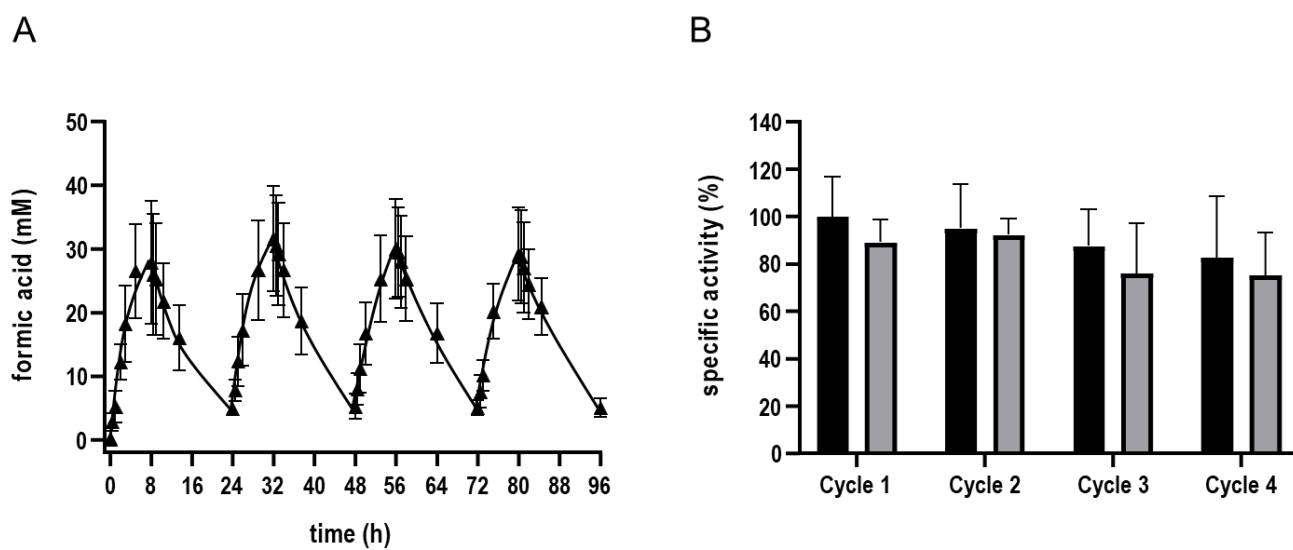
687

688

689

690

691

692 **Figure 3**

693

694

695

696

697

698

699

700

701

702

703

704

705

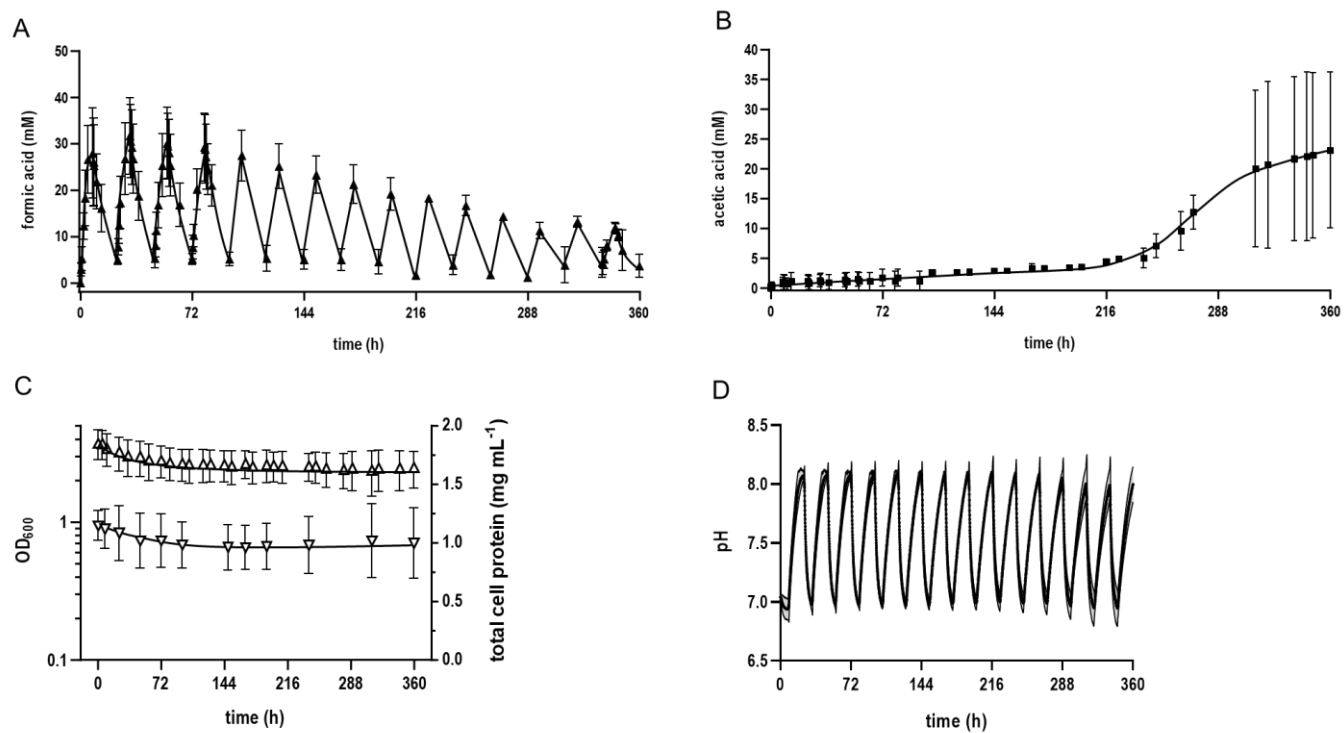
706

707

708

709

710

711 **Figure 4**

712

713

714

715

716

717

718

719

720

721

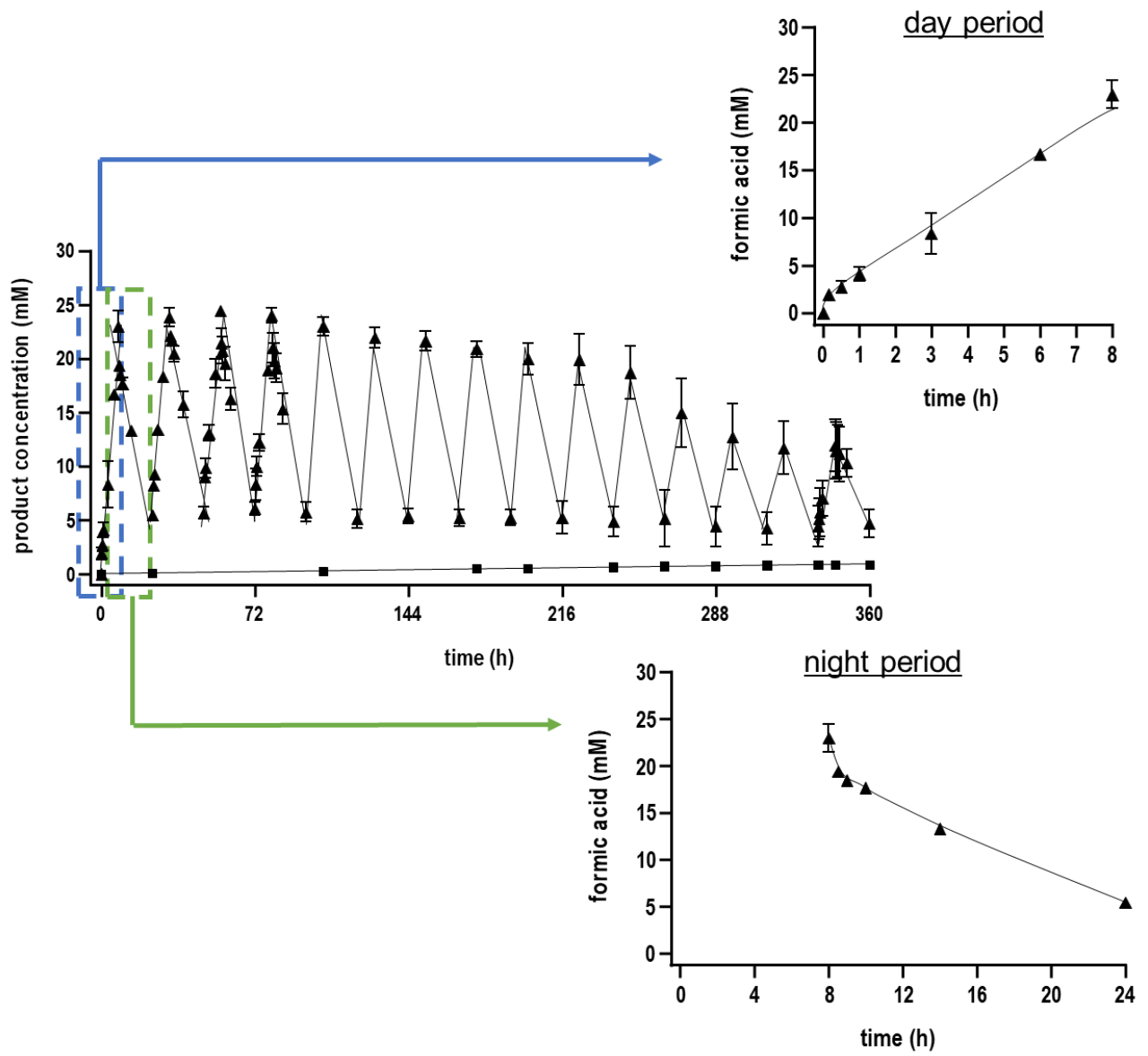
722

723

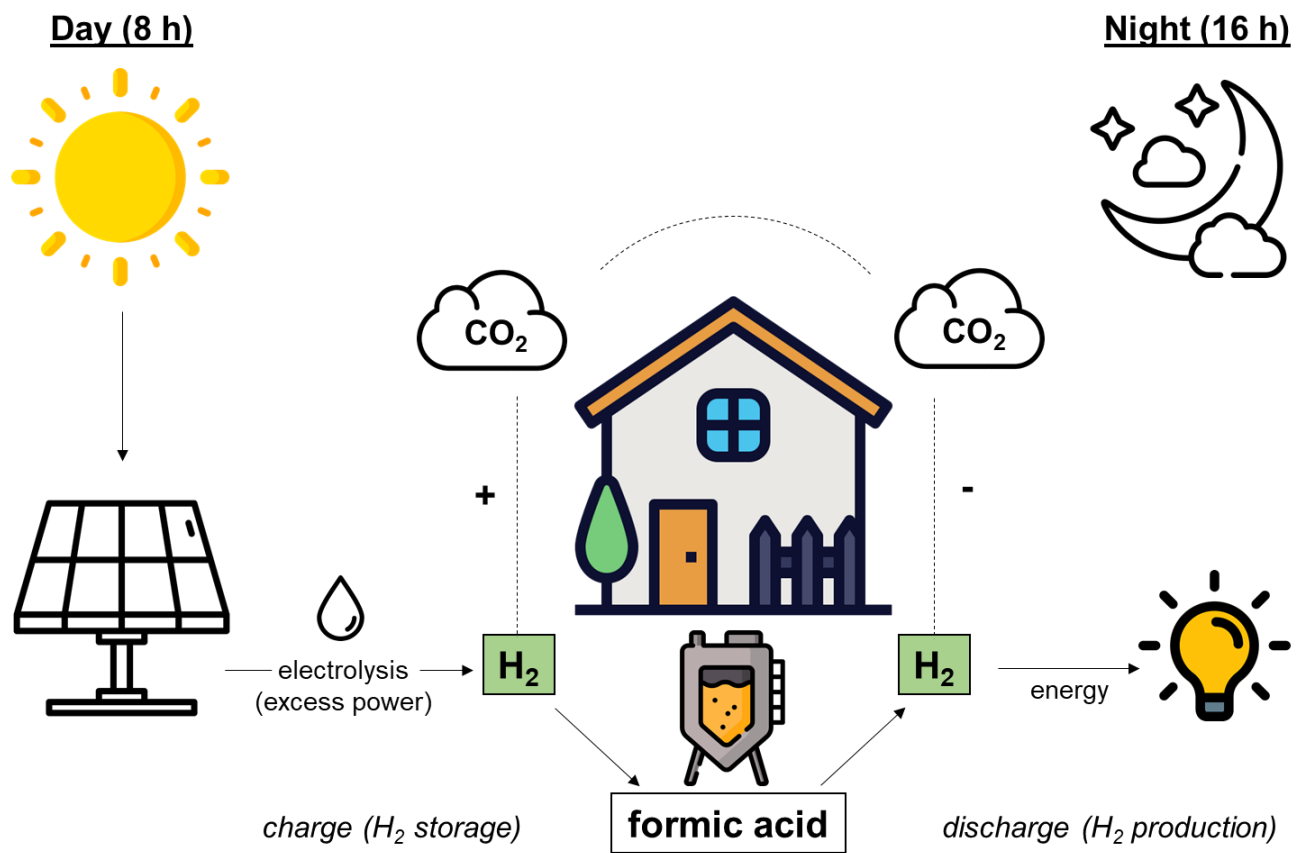
724

725

726

727 **Figure 5**

736

737 **Figure 6**

738

739

740

741

742

743

744

745

746

747

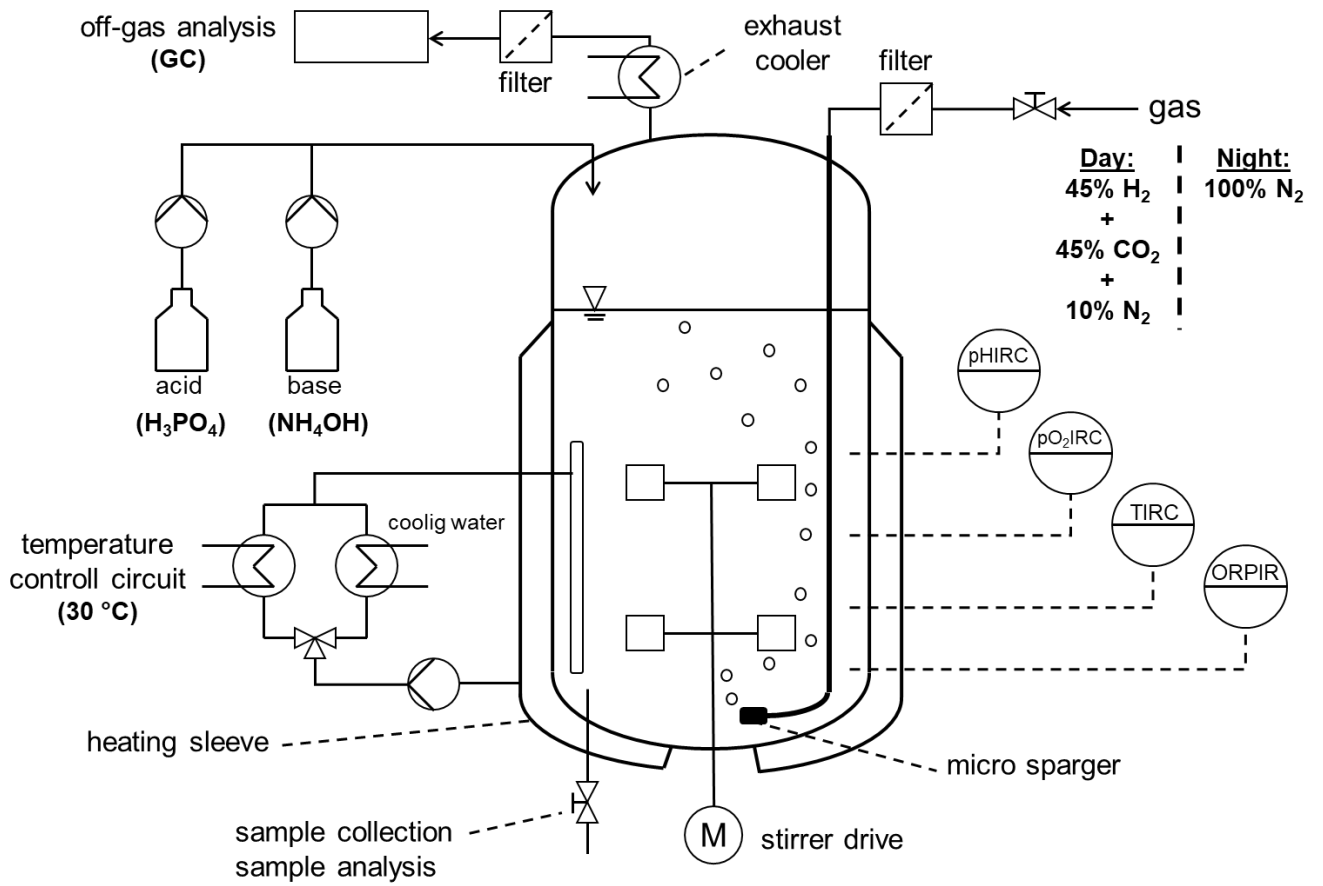
748

749

750

751

752 **Figure 7**



753

754

755

756

757

758

759

760

761

762

763

764

765
766
767
768
769
770
771
772
773
774
775
776
777
778
779
780
781
782
783
784
785
786
787
788
789

Supplementary data

Biological hydrogen storage and release through multiple cycles of bi-directional hydrogenation of CO₂ to formic acid in a single process unit

Fabian M. Schwarz¹, Jimyung Moon¹, Florian Oswald¹ and Volker Müller^{1,2,*}

¹ Department of Molecular Microbiology and Bioenergetics, Institute of Molecular Biosciences, Johann Wolfgang Goethe University, 60438 Frankfurt am Main, Germany

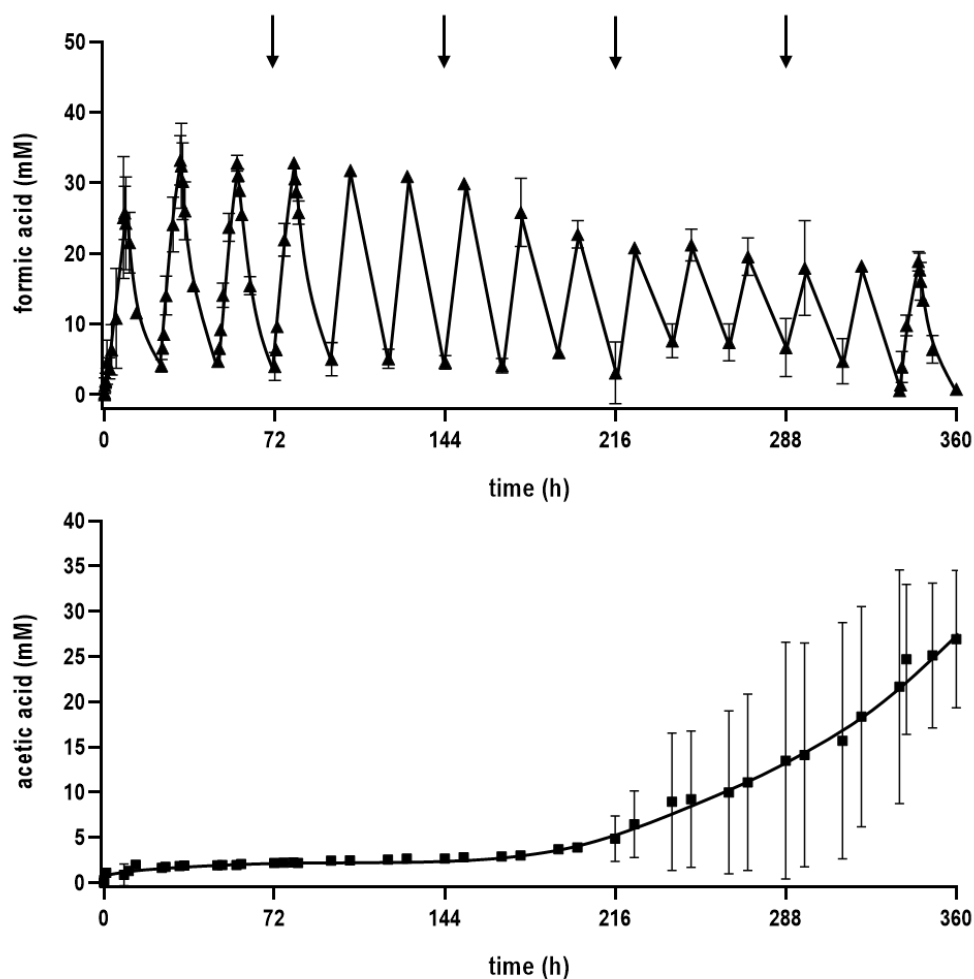
² Lead contact

* Correspondence: vmueller@bio.uni-frankfurt.de

790

791

792



793

794

795 **Figure S1. Long-term application of bi-directional hydrogenation of CO₂ to formic acid in a**796 **bioreactor with repetitive addition of monensin. Shown are A) 15 formic acid formation/oxidation**797 **cycles of the entire process (360 h) and B) corresponding side-product formation profile of acetic acid.**798 Every 72 h, 15 μ M of monensin was added to the bioreactor broth indicated by black arrows. All data799 points are mean \pm SD, N = 3.

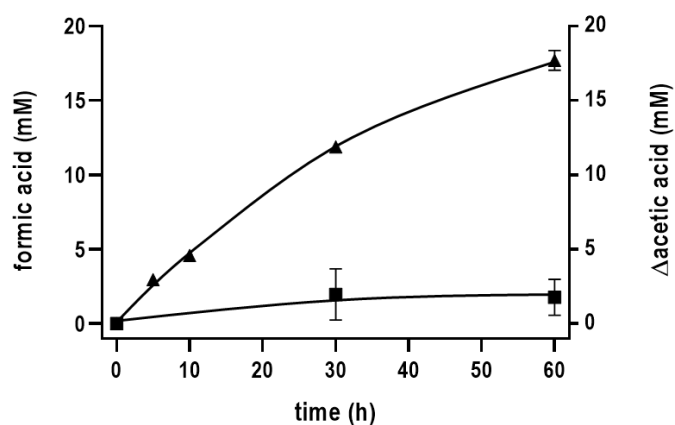
800

801

802

803

804



	serum bottle experiment (fresh buffer)	serum bottle experiment (re-used bioreactor buffer)
Specific formic acid production rate [mmol g ⁻¹ h ⁻¹]	19	29

805

806

Figure S2. Uncoupling effect of used bioreactor buffer on fresh cell suspensions of *A. woodii*.

Serum bottle experiments were performed using the bioreactor buffer (at t_{360h}) relieved from cells by

centrifugation without the addition of new monensin. Freshly prepared *A. woodii* cells were transferred

into the spent buffer to determine their ability to convert H₂ and CO₂ (80:20%, 1 × 10⁵ Pa overpressure)

to formic acid. Due to residual acetic acid in the spent buffer, the difference of formed acetic acid (Δ

acetic acid) to the initial acetic acid is shown. Prior to the start of the experiment 27 mM of acetic acid

was present. Triangles, formic acid; squares, acetic acid. All data points are mean ± SD, N = 2.

813

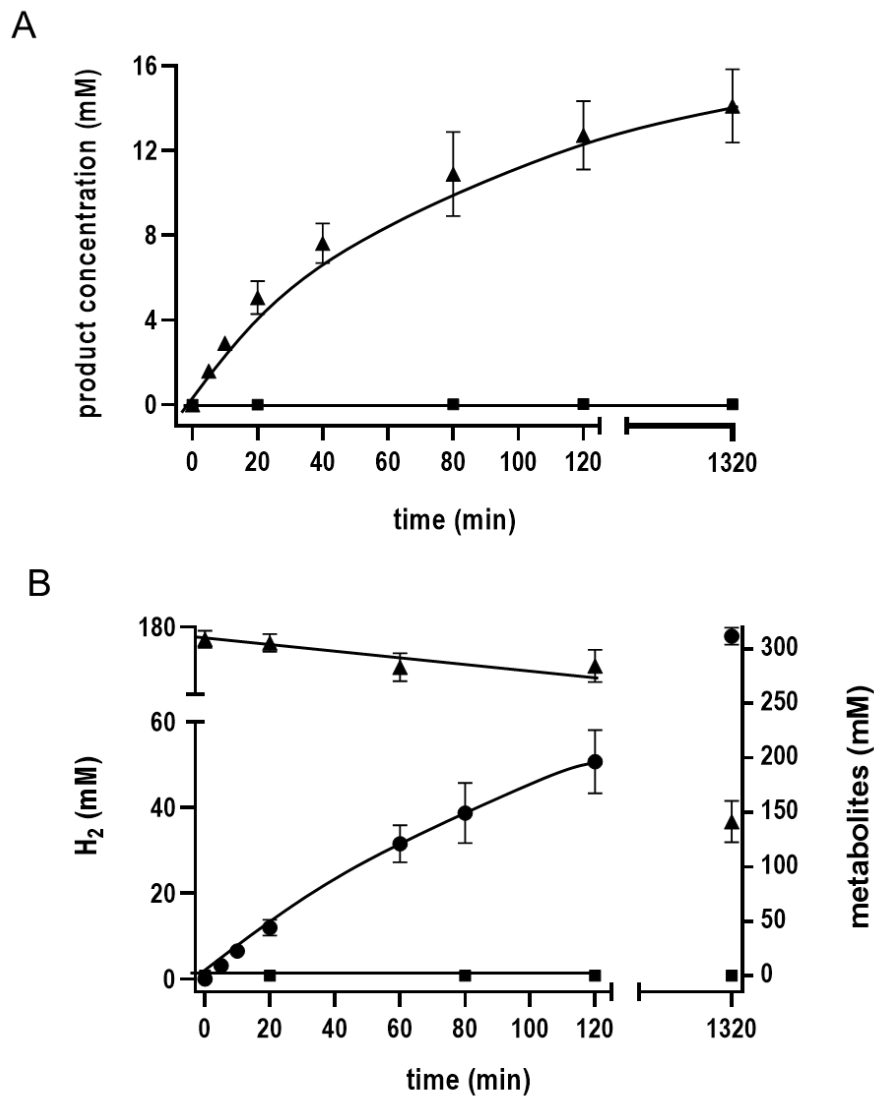
814

815

816

817

818



819

820

821

Figure S3. H₂-dependent CO₂ reduction and formate-driven H₂ production in resting cells of

***A. woodii* $\Delta metVF$.** A) Resting cells (1 mg/mL) of *A. woodii* $\Delta metVF$ were resuspended in K-phosphate

buffer (50 mM K-phosphate, 20 mM KCl, 2 mM DTE, pH 7.0) buffer with a H₂ + CO₂ (80:20%, 1 × 10⁵

Pa overpressure) atmosphere or B) in the same K-phosphate buffer containing 300 mM sodium formate.

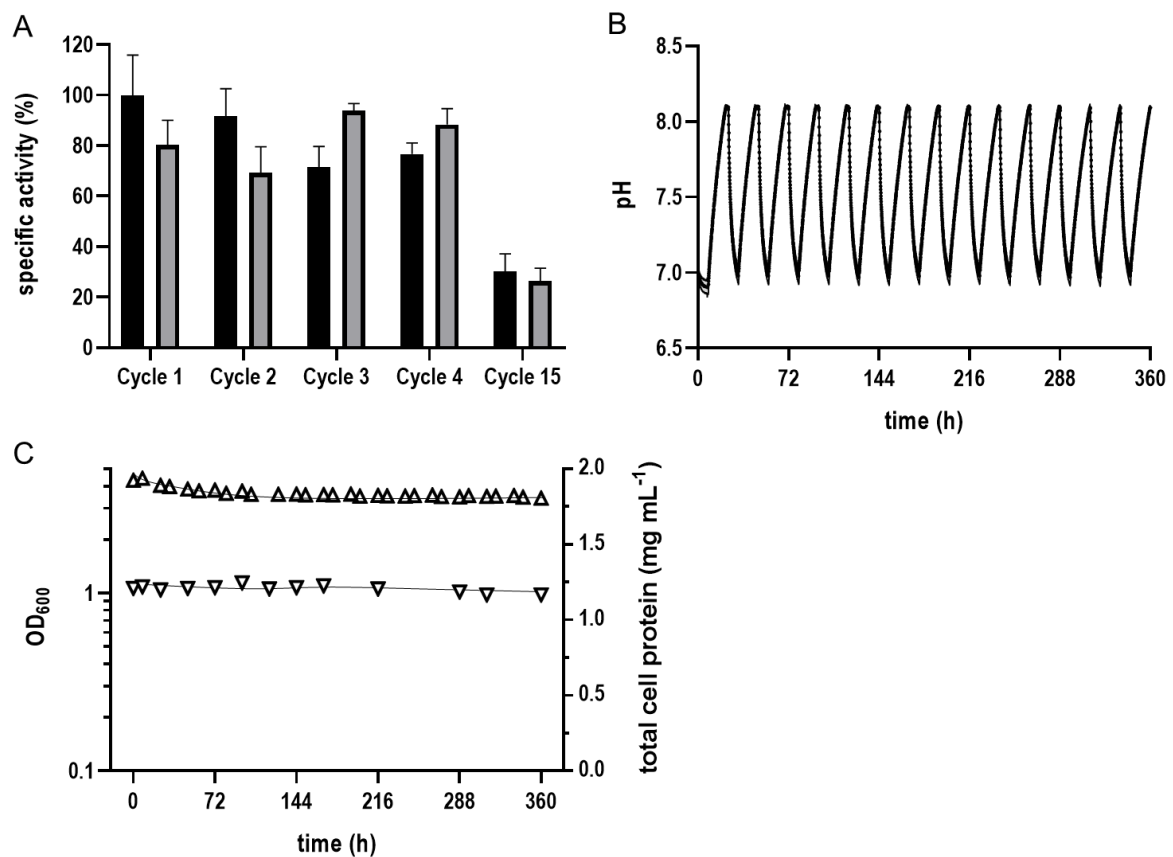
The product and metabolite concentrations were determined. Triangles, formic acid; squares, acetic

acid; circles, H₂. All data points are mean ± SD, N = 3.

826

827

828



829

830

831 **Figure S4. Overview over the catalytic activity, optical density and pH in a bioreactor with**832 ***A. woodii* $\Delta metVF$ cells performing multiple cycles of bi-directional hydrogenation of CO₂ to**833 **formic acid. A) Specific activity of formic acid production (black bars) and formic acid oxidation (grey**834 **bars). 100% of the activity corresponds to a formic acid production rate of 3.0 mmol g⁻¹ h⁻¹ and a formic**835 **acid oxidation rate of 1.7 mmol g⁻¹ h⁻¹. B) pH profile of the entire fermentation. 17 mM of phosphoric acid**836 **and no base was needed as pH correcting agent in the entire process. C) Optical density at 600 nm and**837 **total cell protein concentration. Empty triangles up, optical density at 600 nm; empty triangles down,**838 **total cell protein concentration. All data points are mean \pm SD, N = 3.**

839

840

841

842